Scientific Research Publishing

World Journal of Condensed Matter Physics, 2023, 13, 111-127
https://www.scirp.org/journal/wjcmp
ISSN Online: 2160-6927
ISSN Print: 2160-6919

Compressed H_3S: Fits to the Empirical $H_{c2}(T)$ Data and a Discussion of the Meissner Effect

Gulshan Prakash Malik[1,2], Vijaya Shankar Varma[1,3]

[1]Gurugram, India
[2]Theory Group, School of Environmental Sciences, Jawaharlal Nehru University, New Delhi, India
[3]Department of Physics and Astrophysics, University of Delhi, Delhi, India
Email: gulshanpmalik@yahoo.com, varma2@gmail.com

How to cite this paper: Malik, G.P. and Varma, V.S. (2023) Compressed H_3S: Fits to the Empirical $H_{c2}(T)$ Data and a Discussion of the Meissner Effect. *World Journal of Condensed Matter Physics*, **13**, 111-127.
https://doi.org/10.4236/wjcmp.2023.134008

Received: September 3, 2023
Accepted: October 30, 2023
Published: November 2, 2023

Abstract

Based on μ-, T- and H-dependent pairing and number equations and the premise that $\mu(T)$ is predominantly the cause of the variation of the upper critical field $H_{c2}(T)$, where μ, T and H denote the chemical potential, temperature and the applied field, respectively, we provide in this paper fits to the empirical $H_{c2}(T)$ data of H_3S reported by Mozaffari, *et al.* (2019) and deal with the issue of whether or not H_3S exhibits the Meissner effect. Employing a variant of the template given by Dogan and Cohen (2021), we examine in detail the results of Hirsch and Marsiglio (2022) who have claimed that H_3S does not exhibit the Meissner effect and Minkov, *et al.* (2023) who have claimed that it does. We are thus led to suggest that monitoring the chemical potential (equivalently, the number density of Cooper pairs N_s at $T = T_c$) should shed new light on the issue being addressed.

Keywords

Compressed H_3S, Upper and Lower Critical Fields, Chemical Potential, Generalized Pairing and Number Equations, Coherence Length, Penetration Depth, Meissner Effect

1. Introduction

1.1. Preamble

The discovery of H_2S having a critical temperature (T_c) ≈ 200 K when subjected to a pressure of about 150 GPa [1] marks a significant advance towards the goal of room temperature superconductivity. This feature is now attributed to H_3S which is generally believed to be realized via the reaction $2H_2S \rightarrow (H_3S)^+ + (SH)^-$ [2]. As a consequence, several properties of H_3S have been under intensive investigation, properties such as the values of its gaps (Δs), coherence length (ξ),

lower and upper critical magnetic fields (H_{c1}, H_{c2}), critical current density (J_c) and the London penetration depth (λ_L). Knowledge of these properties enables one to calculate the Ginsberg-Landau parameter (κ) and the critical current density (J_{c1}) due to H_{c1}. Based on the value of J_{c1}, which is one of the criteria among several, Hirsch and Marsiglio (H & M) [3], and references therein, have expressed the opinion that H_3S cannot be classified as a conventional superconductor (SC) because it does not meet the mandatory requirement of displaying the Meissner effect.

The publication of a paper in Nature in 2020 entitled "Room-temperature superconductivity in a carbonaceous sulphur hydride" (C-S-H) by Snider, *et al.* [4] was an exciting development which led Dogan and Cohen (D&C) to carry out a detailed theoretical study of this SC in [5], where they presented some valuable results pertaining to H_3S. While the paper by Snider, *et al.* was subsequently retracted in 2022, the approach followed by D&C for carrying out a comprehensive study of the properties of any SC and their results concerning H_3S remain valid. The template given by D&C, a variant of which we employ here, enables one to obtain at $T = 0$ the values of ξ, Fermi velocity v_F, number density of the charge carriers N_s, λ_L and κ by sequentially employing the following well-known equations:

$$\xi_0 = \sqrt{\frac{\phi_0}{2\pi H_{c2}(0)}} \tag{1}$$

$$v_F(0) = \frac{\pi \Delta_0 \xi_0}{\hbar} \tag{2}$$

$$N_s(0) = \frac{1}{3\pi^2}\left(\frac{m^* v_F^2}{\hbar^2}\right)^{3/2} \tag{3}$$

$$\lambda_L(0) = \sqrt{\frac{m^*}{\mu_0 N_s e^2}} \tag{4}$$

$$\kappa(0) = \frac{\lambda_L(0)}{\xi_0}, \tag{5}$$

where $\phi_0 = 2.0678$ weber, Δ_0 is the value of the gap at $T = 0$, $m^* = \eta m_e$ is the effective mass of the electron, m_e being the free electron mass, $\mu_0 = 4\pi \times 10^{-7}$ h/m_e and e is the electronic charge.

We note that an alternative equation for v_F is

$$v_F = \sqrt{\frac{2\mu}{\eta m_e}}c \quad (\mu \text{ and } m_e \text{ in units of electron-Volts}) \tag{6}$$

D&C's findings about H_3S are:

$$\kappa(0) = 77, \quad \Delta T_c / T_c = 0.15$$

which signify that it is a strongly type II SC.

The line of argument followed by H&M is based on the calculation of the critical current density J_{c1} that comes into play due to the lower critical field H_{c1} and opposes or expels, in accord with Lenz's law, the entry of the magnetic flux into

the interior of an SC when it is subjected to an external magnetic field. The equation for J_{c1} employed by H&M is the London equation

$$J_{c1}(0)=\frac{c}{4\pi\lambda_L(0)}H_{c1}(0), \tag{7}$$

where c is the velocity of light. We note that the value of H_{c1} employed by H&M is based on the demagnetization factor. An alternative expression is

$$H_{c1}=\frac{\phi_0}{4\pi\lambda_L^2}\ln(\kappa) \tag{8}$$

Other features of H_3S that provide a backdrop to the present work are the data for the variation of H_{c2} with temperature given in Mozaffari, *et al.* [6]. These authors also obtained fits to their data by first employing the conventional Ginsberg-Landau theory and subsequently the Werthamer-Helfand-Hohenberg [7] formalism where the temperature dependence of $H_{c2}(T)$ is defined by orbital and spin-paramagnetic effects in the dirty limit. Results of the latter fit that concern us are

T_c of the sample	$H_{c2}(0)$	ξ_0
197 K	88 T	1.84 nm

Following a phenomenological approach, excellent fits to the aforesaid data were also obtained by Talantsev [8] via four equations each of which employed two or more parameters from the following set of properties of H_3S

$$\Sigma 1 = \{T_c, \Delta, \xi, \lambda_L, \text{jump in sp.ht.}\} \tag{9}$$

The values of and $H_{c2}(0)$, $\mu(0)$ and ξ_0 arrived at in [8] are

T_c of the sample	$H_{c2}(0)$	μ_0	ξ_0
191K	100 T	0.47 eV	1.86 nm

1.2. The Scope and the Plan of the Present Paper

We study in this paper the properties of H_3S that were the concern of Talantsev [8], H&M, D&C and Minkov, *et al.* [9] [10] by employing the framework of the chemical potential (μ)-incorporated Bethe-Salpeter equation (BSE). With a superpropagator as its kernel, the BSE leads to a generalization of the BCS equations (GBCSEs) [11] which have been shown to explain several properties of a wide variety of SCs that includes elemental SCs, MgB_2, YBCO, Tl-2212, Bi-2212, $SrTiO_3$, NbN, heavy-fermion and Fe-based SCs. For references to papers where these SCs have been dealt with, see [12].

Insofar as H_3S is concerned, the GBCSEs have been shown to shed light on 1) most of its empirical and inferred features [13], 2) the empirical values of its $J_c(T)$ [14] and 3) the value of its ξ_0 [15]. Further features of H_3S studied here are based on the data for the variation of H_{c2} with temperature given in Mozaffari, *et al.*

The basic premise of our approach, which is an alternative to the approaches followed in [8] and [6], is that the chemical potential $\mu(T)$ of an SC encapsulates most of its physical features such as size, shape, the manner of preparation and the nature of dopants and that it is predominantly responsible for the T-dependent properties of an SC. This idea is of course not new. It was employed earlier

by Eagles [16] in the context of the superconductivity of $SrTiO_3$ by simultaneously considering the μ-dependent gap equation and the equation for μ. Eagle's paper is generally considered to mark the beginning of what is now called the BCS-BEC crossover, which was subsequently dealt with in a similar manner in the work of Leggett [17] by additionally employing scattering length theory (SLT). For a study of cross-over physics without appeal to SLT, we draw attention to [18]. It is notable that while employment of the number equation in [16] [17] [18] in cross-over physics is a matter of course, Schrieffer [19] had made the general remark as early as 1964 that "one must simultaneously solve the gap equation and the constraint condition (*i.e.*, the number equation) to determine Δ_k and μ." By and large, such practice until recently has not percolated into the main stream of the high-T_c SCs for which, in general, the inequality $E_F \gg k\theta$ is not satisfied. To put in perspective the work reported here, we are dealing for the first time with H_{c2} of a system at $T \neq 0$ in accord with Schrieffer's remark.

The μ-, T- and H-dependent core equations via which the $H_{c2}(T)$ and $J_c(T)$ of any SC can be dealt with are given in Section 2. The procedural details of our approach are given in Section 3 where we follow up on [20], in which we gave fits using our approach to two data-sets reported in [6], for the purpose of shedding light on several features associated with

a) H&M's result

$$J_{c1}(0) = 1.87 \times 10^9 \text{ A/cm}^2 \text{ [1]}, \tag{10}$$

which is obtained by employing (7) with the estimates of demagnetizing factor $N = 0.8$, $H_{c1} = 0.48$ T and $\lambda_L = 20.4$ nm, which are based on the experimental set-up of Minkov, *et al.* [9]. The above value of J_{c1} is much greater than that of any other known SC, whether type I or type II, hard or soft;

b) the following more recent results of Minkov, *et al.* [10] for a sample with $T_c \approx 195$ K

$$\xi(10\text{ K}) = 1.85 \text{ nm}, \ \lambda_L(10\text{ K}) = 37 \text{ nm}, \ \kappa(10\text{ K}) = 20, \tag{11}$$

and

$$J_c(30\text{ K}) = 7.1 \times 10^6 \text{ A} \cdot \text{cm}^{-2}. \tag{12}$$

A salient feature of our approach [21] is that, rather than employing any model to calculate J_c, it is based directly on the definition of $J_c = N_s\, e\, v_c$, where e is the electronic charge and v_c the critical velocity of the electrons. As is well known, BCS theory sets the momentum (P) of the centre-of mass of the pairs as zero at the outset, which necessitates the employment of a model for the calculation of J_c based indirectly on its dependence on the applied magnetic field. A virtue of the Bethe-Salpeter formalism is that it enables one to extend BCS to the situation where $P \neq 0$. The equation catering to this situation is one of our core equations.

In the final section we deal afresh with the issue of the Meissner effect in the context of H_3S raised in [3] because the approach followed in this paper differs

[1]Hirsch, J.E. (private communication) agrees that this is the value that should have been given in [3] and not 1.23 x 109 A/cm2.

significantly from the earlier approaches.

The paper includes two appendices for convenience of the reader: The first of these is a glossary of the symbols we have employed and the other comprises two flow charts that give an overview of our procedure.

2. The Core Equations

The generic μ-, T- and H-dependent pairing equation that we employ to calculate $H_c(T)$ or $j_c(T)$ is

$$Eq1(t,h) \equiv 1 - \lambda_{m1} X \int_{z_-(..)}^{z_+(..)} \sum_{n=0}^{N_L(..)} \frac{\tanh\left[A_+(..)\right] + \tanh\left[A_-(..)\right]}{z^2 - 1 + (n+1/2)\dfrac{\hbar\Omega_1(h)}{\mu_1 Y}} = 0, \tag{13}$$

where

$$t = T/T_c\,, \quad h(t) = H_{c2}(T)/H_{c20}$$

$$z_\pm(..) = \sqrt{\frac{Y\rho \pm 1 \mp 1/y}{3Y\rho}}, \; N_L(..) = floor\left[\frac{2k\theta}{3\hbar\Omega_1(h)}\left(1 + Y\rho - 1/y\right) - \frac{1}{2}\right]$$

$$A_\pm(..) = \frac{\rho\theta Y}{2tT_c}\left[z^2 - 1 + (n+1/2)\frac{\hbar\Omega_1(h)}{\mu_1 Y} \pm \frac{1}{\mu_1 Y y}\right]$$

$$\mu_1 = \rho k\theta, \; y = k\theta/\alpha\,, \; \alpha = |\boldsymbol{P}||\boldsymbol{p}|\cos(\boldsymbol{P},\boldsymbol{p})/2m^*\,, \; m^* = \eta m_e$$

$$\Omega(h) = \Omega_0 h H_{c2}(0)/\eta\,, \; \Omega_0 = e/m_e c$$

θ is the Debye temperature (DT) of the ions that cause pairing and μ_1 the chemical potential at $t = 1$; $\boldsymbol{P}$ is the momentum of the pairs in the lab frame, $\boldsymbol{p}$ the relative momentum of their constituents in the center-of-mass frame and m^* is the effective mass of an electron, m_e being the free electron mass; the unit for the applied field is Gauss.

For (X, Y) in (13), we shall employ the following values

$$X = 1, \; Y = 1 \tag{14}$$

$$X = Y = q(t) \tag{15}$$

$$X = \frac{1}{\sqrt{q}}\frac{h}{h_1}, \; Y = q \tag{16}$$

Substitution of (14) into (13) yields the value of the interaction parameter λ_{m1} with the input of θ, ρ, η, $t = t_1$ and $h_1 = H_1/H_{c20}$, H_1 being the value of the self-field at $t = t_1$ in the absence of any applied field and $\boldsymbol{P} = 0$ ($y = \infty$).

Substitution of (15) into (13) determines how λ_{m1}, μ_1 and h_1 change with t. It has been shown [20] that each of the following models for $q(t)$ provides an excellent fit to the data of Mozaffari, *et al.*:

$$\begin{aligned} q(t) &= 1 + a_0(1-t) && \text{(i)} \\ &= 1 + a_0\left(1 - t^{a_1}\right) && \text{(ii)} \\ &= 1 + a_0\left(1 - t^2\right)^{a_2}. && \text{(iii)} \end{aligned} \tag{17}$$

However, these fits came with the caveat that $\mu(0) = q(0)\rho k\theta > 250$ eV for all these models, in stark contrast with its value < 1 eV noted in (9). Because any value of $\rho < 1$ causes the limit z_- in (13) to become pure imaginary and leads to complex roots, the fits in [20] were obtained by employing $\rho = 1$. In order to seek fits that also lead to $\mu(0)$ of the desired order, we stipulated that $z_- = \mathrm{Re}\left(\sqrt{(\rho-1)/3\rho}\right)$ in (13) order to employ values of $\rho < 1$. Remarkably, we thus found that innumerable such values also lead to fits as good as those obtained earlier. Because model (17iii) had led to the least value of $\mu(0)$, this is the model we adopt for values of $T < T_c$ which enable us to shed light on the values of J_c noted in (10) and (12) by employing the number equation given below. Because of the employment of (17iii), we call this the (a_0, a_2) approach.

Interestingly, the J_c values of both H&M and Minkov, *et al.* [10] can also be addressed by appealing simultaneously to the number equation and (13) with the choice of X, Y as in (16). This approach leads to the values of (q, y) corresponding to each pair of (h, j_c) at any T; we therefore call it the (q, y) approach which enables one to calculate several T-dependent properties of the SC such as N_s, ξ, etc. The derivation of (13) with X and Y as in (16) has been given in [21].

Our other core equation is the number equation derived in [22]

$$N_s(t,h) = C\left(hH_{c2}\right)^{3/2}\int_0^{\sqrt{L(t,h)}}\left[\sum_{n=0}^{N_m(t,h)}\{....\}\right]\mathrm{d}z,$$
$$\{....\} = \left\{1-\tanh\left(\frac{\hbar\Omega(h)}{2ktT_c}\left[n+1/2+z^2-\frac{q(t)\mu_1}{\hbar\Omega(h)}\right]\right)\right\} \tag{18}$$

where

$$C = 2.1213\times10^9,\ L(t,h) = \frac{1}{3}\frac{k\theta\left[\rho q(t)+1\right]}{\hbar\Omega(h)}$$
$$N_m(t,h) = floor\left[\frac{2}{3}\frac{k\theta\left[\rho q(t)+1\right]}{\hbar\Omega(h)}-\frac{1}{2}\right].$$

Since we employ (18) in lieu of (3), it is prudent to compare the results one obtains when the inputs employed for both the equations are nearly the same. Insofar as the latter equation is concerned, for C-S-H it yields $N_s = 5 \times 10^{27}$ m^{-3} [5] for $\eta = 1$, $E_F = 1.06$ eV (which follows from $v_F = 6.1 \times 10^5$ m/s), $T = 0$ and $H = 0$. For the same values of η and E_F, $T = 10^{-6}$ K and $H = 300$ G (which is the *sf* that exists in the absence of an applied field), (18) yields $N_s = 1.75 \times 10^{27}$ m^{-3}.

Remark: With the employment of (18) in the following in mind, we note that the result $N_s = 1.75 \times 10^{27}$ m^{-3} remains unchanged whether $H_{c2} = 0.03$ or 120 T for any value of the temperature. It is notable in this context that $J_c = 0$ at $H = H_c$ because $v_c = 0$ and not because N_s given by (18) vanishes.

The equation for the critical velocity v_c in terms of (q, y) is [21]

$$v_c(...) = \frac{c}{2y}\sqrt{\frac{6k\theta}{q\rho\eta m_e}}, \tag{19}$$

whence the number equation may be written as

$$1-\frac{J_c(..)}{eN_s(..)v_c(..)}=0. \tag{20}$$

3. Fits to an Empirical Data-Set of Mozaffari, *et al.* and a Study Pertaining to the Results in (10)-(12)

We undertake in this section the task of shedding light on the results given in the above-noted equations. For this purpose, we employ the $H_{c2}(T)$ data of Mozaffari, *et al.* which covers the range T_c = 191 K to 105.1 K. Because we need the values of $\mu(t)$ [= $q(t)\mu_1$] and H_{c2} at 0, 10 and 30 K, vide (10 - 12), we now need a model for $q(t)$ that provides a fit to the data and thence to the values of μ and H_{c2} at any specific temperature.

3.1. Procedure for Finding a Fit to Any Set of $H_{c2}(T)$ Values

a) Resolve the Debye temperature (DT) of H_3S given by Talantsev [23] as $\theta(H_3S)$ = 1531 K into the DTs of its constituents by employing the double-pendulum model [24], whence

$$\theta_H=1983.2\text{ K},\ \theta_S=174.5\text{ K}. \tag{21}$$

b) Both of these DTs are *needed* [13] for an explanation of the empirical value of the T_c of H_3S and its inferred gap-values of about 40 meV and 28 meV because the 1-phonon exchange mechanism (1PEM) per se due either to the H or the S ions violates the Bogoliubov constraint [11]. However, since a magnetic field considerably weakens the strength of the interaction, it turns out that the data being addressed here can be dealt with via the consideration of the *H* ions alone.

c) With $\theta=\theta_H$, solve $Eq1(t, h)$, vide (13), to obtain λ_{m1} for any chosen value of ρ with the input of η = 2.76 (following [8] where it was shown to lead to reasonable values of several parameters), t = 1, $X=Y=1$, $y=\infty$, $h=300/H_{c20}=3\times10^{-4}$, where 300 G is the self-field *sf* and $H_{c20}=10^6$ G (chosen for convenience because it enables one to look for numerical solutions near $h\approx1$).

d) Solve $Eq1(t_1, h_1)$ and $Eq1(t_2, h_2)$, vide (13), with X and Y as in (15) and $y=\infty$ to fix the constants a_0 and a_2 in the employed model (17iii) by choosing two (t, h) points from the empirical data of 23 such points. For all values of ρ that we employed, the points chosen were

$$\left(t_1=145/T_c, h_1=30.27/H_c\right)\ \text{and}\ \left(t_2=105/T_c, h_2=61.49/H_c\right). \tag{22}$$

3.2. On H&M's Result Noted in (10)

3.2.1. The (a_0, a_2) Approach

H&M have given the value of $J_{c1}(0)=1.87\times10^9$ A/cm^2 as corresponding to H_{c1} = 0.48 T and λ_L = 20.4 nm. The issues we address here are a) Can these results be validated via the (a_0, a_2)-approach? b) If so, what are the values of several other parameters such as v_F, ξ and κ corresponding to this triplet?

A salient feature of our approach is that all the results it leads to via a chain of calculations depend only on three parameters, viz., ρ (which determines the

chemical potential at $t = 1$), η and *sf*. Among these, by far the most important parameter is ρ [20]. For this reason, while seeking to obtain H&M's value of $J_{c1}(0)$, we kept the values of η and the *sf* fixed at 2.76 and 0.03 T, respectively, and varied only ρ. We thus found that H&M's triplet follows by employing, at $T = T_c$, the value of ρ as 0.164, which we arrived at after carrying out calculations for many values of ρ. The detailed results are as follows.

$$\rho = 0.164,\ \mu_1 = 2.80\times10^{-2}\ \text{eV},\ \eta = 2.76,\ h = sf = 300\ \text{G},\ t = 1$$

$$\text{At T} = 10^{-3}\ \text{K}:\ \mu = 9.88\ \text{eV},\ H_{c2} = 332.2\ \text{T},\ \lambda_m = 2.206\times10^{-3},\ N_L = 479 \quad (23)$$

$$\text{At T} = 10\ \text{K}:\ \mu = 9.85\ \text{eV},\ H_{c2} = 145.1\ \text{T},\ \lambda_m = 2.199\times10^{-3},\ N_L = 1095 \quad (24)$$

Obtained for either of the above values of μ via (6):

$$v_F = 1.12\times10^6\ \text{m/s}$$

Obtained via (2), with $\Delta = 38$ meV, (18), (4) and (5), respectively,

$$\xi = 6.18\ \text{nm},\ N_s = 1.91\times10^{29}\ \text{m}^{-3},\ \boldsymbol{\lambda_L = 20.2\ \text{nm}},\ \kappa = 3.27$$

Obtained via (8): $\boldsymbol{H_{c1} = 0.48\ \text{T}}$; obtained via (7): $\boldsymbol{J_{c1} = 1.88\times10^9\ \text{A/cm}^2}$

3.2.2. The (q, y) Approach

In this approach, we seek to find the value of ρ which leads with the input of J_{c1} and H_{c1} to the value of the third member of the H&M's triplet, i.e., λ_L, as ≈ 20.4 nm at 10 K. Since the H&M's triplet is given at $T = 0$ and Minkov, *et al.* have given the values of ξ, λ_L, and κ at $T = 10$ K and the values of J_{c1} at 30 K, a meaningful comparison of various other parameters associated with these necessitates that we should first obtain the value of the H&M's triplet at $T = 10$ K from its value at $T = 0$. We have done so by appealing to the 2-fluid theory and found that, to an accuracy of second place after the decimal, we need to change only J_{c1} from 1.87×10^9 to 1.86×10^9 A/cm^2. After repeating the chain of calculations for several value of ρ, we were led to $\rho = 37.8$ as the value which leads to the desired value of λ_L. The details of this exercise which also gives the values of several other parameters associated with H&M's triplet at 10 K are given below.

$$\rho = 37.8,\ \mu_1 = 6.46\ \text{eV},\ \eta = 2.76,\ h = sf = 300\ \text{G},\ t = 1$$

Obtained via (13) with $X = Y = 1$: $\lambda_{m1} = 8.273\times10^{-7}$, $N_L = 3513054$

Obtained by simultaneously solving (20) and (13) for $T = 10$, $t = 10/T_c$ with X, Y as in (16) and the input of

$$\boldsymbol{H_{c1} = 0.48\ \text{T}},\ J_{c1} = \boldsymbol{1.86\times10^9\ \text{A/cm}^2}$$

$$q = 1.5249,\ y = 27.646,\ \mu = 9.851\ \text{eV},\ \lambda_m = 1.072\times10^{-5}$$

Obtained via the equations noted above for the (a_0, a_2) approach

$$v_F = 1.12\times10^6\ \text{m/s},\ \xi = 6.17\ \text{nm},\ N_s = 1.90\times10^{29}\ \text{m}^{-3}$$

$$v_c = 6\times10^4\ \text{m/s},\ \boldsymbol{\lambda_L = 20.22\ \text{nm}},\ \kappa = 3.27$$

Our findings related with H&M's values of J_{c1}, H_{c1} and λ_L will be discussed below.

3.3. On Minkov, *et al.*'s [9] Result Noted in (11)-(12)

3.3.1. The (a_0, a_2) Approach

As above, we begin with an assumed value of $\rho < 1$, employ $\eta = 2.76$ and $sf = 300$ G and solve (13) to obtain the value of λ_{m1} at $t = 1$. We then employ model (17iii) and find the values of a_0 and a_2. This is followed up by the chain of calculations as before leading finally to a value of κ. Repeating this procedure by varying ρ, we were able to find the values of this parameter that lead to $\kappa \approx 20$ as noted in (11). Given in **Table 1** are five values of ρ that lead to a value of κ in the desired ballpark and the values of various other corresponding parameters.

Given in **Figure 1** is the fit to the empirical data provided by model (17iii) for $\rho = 0.065$ which leads to $\kappa = 19$.

3.3.2. The (q, y) Approach

Let us first note that by adopting the values of the diameter (d), thickness (th) and the trapped magnetic flux [m_{trap}(30 K)] of their sample as 85 μm, 2.8 μm and 1.60×10^{-8} A m^2, respectively, Minkov *et al.* obtained the result noted in (12) as follows:

$$J_c\left(30\text{ K}\right) = \frac{3}{\pi}\frac{m_{trap}\left(30\text{ K}\right)}{d}\left(\frac{2}{th}\right)^3 = 7.1\times 10^6\text{ A}/\text{cm}^2. \tag{25}$$

Next, we note that if we employ the values of λ_L and κ at $T = 10$ K as given in (11), then we are led to the corresponding value of H_c via (8) as

$$H_{c1} = 0.36\text{ T}. \tag{26}$$

We now follow the procedure given above by employing (25) and (26) in lieu of H&M's values of J_c and H_{c1}. Given in **Table 2** are the results of this exercise for a few select values of ρ.

4. Summing Up

1) Based on the premise that the variation in $H_{c2}(T)$ is caused predominantly by $\mu(t)$, we have obtained in this paper a fit to an empirical $H_{c2}(T)$ data-set of Mozaffari, *et al.* by employing (13). While excellent fits to the same data were obtained earlier by Talantsev [8] via four phenomenological equations each of which employed two or more parameters from the set Σ_1 in (9), our approach has been shown to lead to a similar fit, vide **Figure 1** which relates $H_{c2}(T)$ with a set of variables altogether different from Σ_1, viz.,

$$\Sigma_2 = \left\{\theta, \lambda_m\left(T\right), \mu\left(T\right), L_N\left(T\right)\right\}. \tag{27}$$

For the variation of $\mu(t) = \mu_1 q(t)$ ($\mu_1 = \rho k\theta$), the model we employed for $q(t)$ was specified in (17iii). The work in [20] and this paper shows that while almost equally good fits to the same data can be obtained by numerous values of ρ, the values of v_F, ξ and λ_L, etc., that they lead to are different.

2) The issue of the Meissner effect in the context of H_3S was addressed by dealing with H&M's values of the triplet $\{J_{c1}, H_{c1}, \lambda_L\}$ and Minkov, *et al.*'s values of ξ, λ_L and κ at 10 K and j_c at 30 K by employing both the (a_0, a_2) and the (q, y)

Table 1. Values of various parameters of H_3S at $T = 10$ K obtained by following the procedure of the (a_0, a_2) approach given in Section 3.2.1.

$t=1$		Model (17iii)				$t=10/T_c$				
ρ $\mu_1=\rho k\theta$ eV	η λ_{m1} 10^{-5}	a_0 a_2	$\mu=q\mu_1$ eV	λ_m 10^{-3}	H_{c2} N_L	v_F m/s 10^5	ξ nm	N_s m^{-3} 10^{28}	λ_L nm	κ
0.071 0.012	2.76 1.177	215.0 1.0939	2.613	2.534	151.7 291	5.77	3.18	2.79	52.8	17
0.065 0.011	2.76 1.248	205.9 1.0899	2.285	2.568	152.0 256	5.41	2.98	2.32	58.0	19
0.055 0.0094	2.76 1.392	190.6 1.0857	1.796	2.658	154.3 202	4.78	2.64	1.65	68.9	26
0.050 0.0085	2.76 1.478	181.9 1.0783	1.558	2.696	154.8 177	4.46	2.46	1.36	76.0	31
0.050 0.0085	3.20 1.275	181.9 1.0783	1.558	2.325	154.9 205	4.14	2.29	1.69	73.1	32

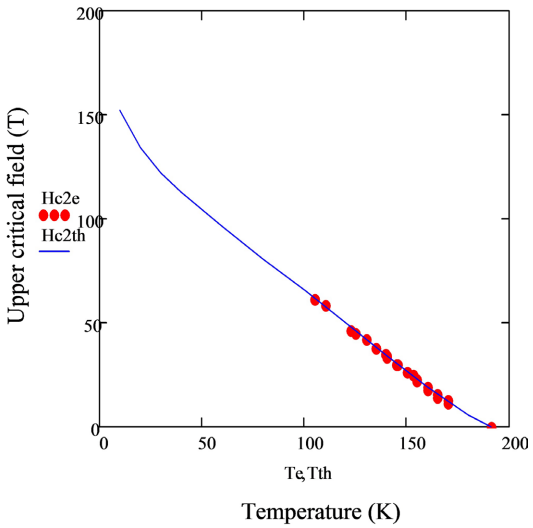

Figure 1. For the sample with $T_c = 191$ K, the variation of the upper critical field of H_3S with temperature obtained via (13) by employing $\rho = 0.065$ and $q(t)$ as in (17iii). The filled circles are the plot of the empirical values.

approaches. We note that in the former approach, the equation which we solve to obtain the value of H_{c2} for any value of temperature has multiple roots. Since these roots are extremely close to each other, one may employ any one of them for the calculation of any parameter dependent on them. An example: for $\rho = 0.164$, there are three roots at $h = 1.4583$, 1.4593 and 1.4603.

3) Re: H&M's values of the triplet $\{J_{c1}, H_{c1}$ and $\lambda_L\}$

a) The (a_0, a_2) approach. Beginning with $\rho = 1$, $\eta = 2.76$ and $sf = 300$ G and employing model (17iii) for $q(t)$, we determined via (13) the values of a_0 and a_2 that provide a fit to the $H_{c2}(T)$ data of Mozaffari, *et al.* With $H_{c2}(t)$ and $\mu(t) =$

Table 2. Sample with T_c = 191 K. Values of λ_{m1} obtained by solving (13) with the inputs η = 2.76, sf = 300 G. Inputs for (13) to obtain λ_{m1}: X=1, Y = 1, t = 1, $h = 300/H_{c20}$ ($H_{c20} = 10^6$ G). Values of (q, y) obtained by solving (13) and (20) simultaneously, with X, Y as in in (16), and the inputs $t = 10/T_c$, $h = 0.36 \times 10^4/H_{c0}$, J_c(10 K) = 7.27 × 10⁶ A/cm² (obtained from J_c(30 K) = 7.1 × 10⁶ A/cm²). Equations for the calculation of v_F, ξ, N_s, λ_L and κ as given in the text.

At $t=1$			At $t=10/T_c$			
ρ μ_1 eV	λ_{m1} $\times 10^{-6}$ N_{L1}	q y	μ_2 (eV) λ_{m2} $\times 10^{-6}$ N_{L2}	v_{F2} $\times 10^5$ (m/s) ξ_2 (nm)	$N_{s1} = N_{s2}$ $\times 10^{28}$ (m^{-3}) λ_L (nm)	κ
8.5 1.453	1.025 860154	4.846 5105	7.039 5.590 318321	9.48 5.22	11.6 25.9	4.96
7.7 1.316	1.042 787720	4.943 4731	6.505 5.623 294778	9.10 5.02	10.4 27.4	5.46
4.6 0.786	1.135 507038	5.52 3213	4.339 5.796 199112	7.44 4.10	5.75 36.8	8.98
3.0 0.513	1.220 362170	6.064 2350.3	3.109 5.947 144786	6.29 3.47	3.56 46.80	13.5
2.0 0.342	1.301 271627	6.543 1737.7	2.235 6.104 106269	5.34 2.94	2.23 59.1	20.1
1.75 0.299	1.324 248991	6.645 1562.5	1.987 6.162 95274	5.03 2.77	1.89 64.2	23.1

$\mu_1 q(t)$ known,we were enabled to sequentially obtain, at any value of t, the values of v_F, ξ, N_s, λ_L,H_{c1} and finally J_{c1} via equations that have been specified in Section 3.2.1. Because the value of J_{c1} we obtained for ρ = 1 disagreed with H&M's value, we repeated the chain of calculations by varying ρ, till we found that ρ = 0.164 leads to J_{c1} = 1.88 × 10⁹ A/cm², which is very close to H&M's value of 1.87 × 10⁹ A/cm². Corresponding to this value of J_{c1}, the values of H_{c1} = 0.48 T and λ_L = 20.2 nm were found to be in remarkable agreement with the H&M's values, viz., 0.48 T and 20.4 nm, respectively. These results provide a validation of the H&M's triplet because they have been obtained via an altogether different approach without employing the value of any member of it as an input. However, the values of v_F = 1.12 × 10⁶ m/s, ξ = 6.18 nm corresponding to the triplet are not in accord with current wisdom because it is believed that the upper limit of the universal Fermi velocity for hydrides is 3.8 × 10⁵ m/s and ξ lies in the range 1.2 - 3 nm. Besides, the value of and κ = 3.27 is much lower than several estimates of it.

b) The (q, y) approach. In this approach, by simultaneously solving (13) and

(20) for q any $y$with the input of the J_{c1} and H_{c1} values of the H&M's triplet, we sought to obtain the value of ρ which leads to a value of λ_L at $T = 10$ K close to its value in the triplet. By repeating this process for several values of ρ, we found its desired value to be ≈ 37.8, *i.e.*, $\mu\,(T = T_c) = 6.46$ eV. The values of v_F, ξ, λ_L and κ at $T = 10$ K corresponding to it were found to be, respectively, 1.12×10^6 m/s, 6.18 nm, 20.22 nm and 3.27—which are not too different from their values in the (a_0, a_2) approach.

4) Re: Minkov, *et al.*'s values of ξ, λ_L and κ at 10 K

a) The (a_0, a_2) approach. Our objective now was to find the value of ρ for which the chain of calculations culminates in the value of κ rather than J_c. Beginning with $\rho = 1$ and repeating the procedure with progressively lower values, we found that $\rho = 0.065$ ($\mu_1 = 0.011$ eV) leads to $\kappa = 19$, which is very close to Minkov, *et al.*'s value of 20. However, our values of $\xi = 2.98$ nm and $\lambda_L = 58.0$ nm were greater than Minkov, *et al.*'s values, viz., 1.85 nm for the former and 37 nm for the latter. Besides, the corresponding value of $v_F = 5.41 \times 10^5$ m/s was also found to exceed its universal upper limit. We were hence led to explore if we could simultaneously obtain a lower value for each of these parameters by a different choice of ρ. As is seen from Table 1, we could not succeed because we found that while increasing the value of ρ decreases λ_L and ξ, it increases the values of v_F and ξ. Decreasing the value of ρ had the opposite effect.

b) The (q, y) approach. From Minkov, *et al.*'s value of J_c (30 K) = 3.1×10^6 A/cm^2, we estimated via the 2-fluid theory the value of J_c (10 K) to be 3.27×10^6 A/cm^2. Employing it together with H_c (10 K) = 0.36 T, vide (26), we could obtain the values of q and y corresponding to any value of ρ by simultaneously solving (13) and (20). The values of v_F, ξ, λ_L, κ, etc., for six triplets of $\{\rho, q, y\}$ are given in Table 2. Again, while our values of κ for two of these triplets matched Minkov, *et al.*'s value, the values of λ_L and ξ did not. Also, our value of v_F exceeded its universal upper limit.

5) Concluding remarks

a) Some of the values of κ that we obtained via two different approaches are not as alarming as 77 given by D&C.

b) Re: the difference between our values of ξ and λ_L and those of Minkov, *et al.* corresponding to the same value of $\kappa \approx 20$, we note that in both of our approaches the values of all the parameters that we calculated depend predominantly on ρ which determines the chemical potential at $T = T_c$; the other two parameters that need to be specified at the beginning, viz., η and *sf* were not varied. It is plausible that by fine tuning the values of η and *sf*, the said disagreement is reduced. We draw attention in this context to the last row in Table 1 where changing η from 2.76 to 3.20 is seen to have the effect of reducing v_F, ξ and λ_L and marginally increasing κ. Similarly, changing *sf* from 300 to 350 G was found to decrease v_F and ξ and λ_L and to increase κ.

c) Our finding that there are two values of μ- one obtained via the (a_0, a_2) approach and the other via the (q, y) approach, corresponding to the H&M's or Minkov, *et al.*'s triplet of $(J_{c1}, H_{c1}, \lambda_L)$ is reminiscent of $SrTiO_3$, the plot of the T_c

of which against concentration has a dome-like structure [16] [11].

d) Drawing attention to (23) and (24), we note that as the temperature is lowered from 10 K to 10^{-3} K, the increase in the value of μ from 9.85 eV to 9.88 eV is accompanied by a disproportionate increase in the value of H_{c2} from 145 T to 332 T. This super-linear upturn of the H_{c2} curve at low values of temperature is also seen in **Figure 1** and is an unfamiliar feature. However, recent plots of the trapped magnetic moments in hydrides given by Minkov, *et al.* [10] show a similar behavior, vide upper panels c and d in their Figure 1 and panels a and b in Figure 4. Although the authors have attributed this feature to sulphur, the fact nonetheless remains that it has been observed in an experiment concerned with H_3S.

e) We would like to emphasize that the above feature of $H_c(T)$ close to 0 K plays no role in our work other than providing the values of μ at $T \approx 0$ and 10 K. This is so because $H_{c2}(T)$ is employed only while using the number equation where its value is immaterial, vide the Remark below (18).

f) Salient features of our findings in this paper are

1) we have shown that the Hirsch and Marsiglio's triplet of $\{J_{c1}, H_{c1}, \lambda_L\}$ leads to values of v_F and ξ that are considerably greater than their currently believed upper limits, and to a value of κ which is much lower than several available estimates of it as in [5] and [8].

2) while we were led via two different approaches to the values of κ in the same ballpark as its value reported by Minkov, *et al.* [10], our values of λ_L and ξ corresponding to it differ from their values. We also believe to have shown that this is an issue which can be resolved by monitoring μ (equivalently, N_s) at $T = T_c$ which, via the chain of calculations carried out in this paper, predominantly determines a host of the properties of the SC, including H_{c1} and J_{c1} which are associated with the Meissner effect.

g) We conclude by noting that the repository of knowledge gained from the study of the conventional SCs may not always be a good guide in dealing with SCs like compressed H_3S because none of the former category of SCs has been studied at such high pressures as the latter.

Conflicts of Interest

The authors declare no conflict of interest.

References

[1] Drozdov, A.P., Eremets, M.I., Troyan, I.A., Ksenoafontov, V. and Shylin, S.I. (2015) Conventional Superconductivity at 203 Kelvin at High Pressure in Sulfur Hydride System. *Nature*, **525**, 73-76. https://doi.org/10.1038/nature14964

[2] Gordon, E.E., *et al.* (2016) Structure and Composition of the 200 K-Superconducting Phase of H_2S at Ultrahigh Pressure: The Perovskite (SH^-) (H_3S^+). *Angewandte Chemie International Edition*, **55**, 3682-3684. https://doi.org/10.1002/anie.201511347

[3] Hirsch, J.E. and Marsiglio, F. (2022) Clear Evidence against Superconductivity in Hydrides under High Pressure. *Matter and Radiation at Extremes*, **7**, Article ID:

058401. https://doi.org/10.1063/5.0091404

[4] Snider, E., *et al*. (2020) RETRACTED ARTICLE: Room-Temperature Superconductivity in a Carbonaceous Sulfur Hydride. *Nature*, **586**, 373-377. https://doi.org/10.1038/s41586-020-2801-z

[5] Dogan, M. and Cohen, M.L. (2021) Anomalous Behavior in High-Pressure Carbonaceous Sulfur Hydride. *Physica C*: *Superconductivity and Its Applications*, **583**, Article ID: 1353851. https://doi.org/10.1016/j.physc.2021.1353851

[6] Mozaffari, S., *et al*. (2019) Superconducting Phase Diagram of H3S under High Magnetic Fields. *Nature Communications*, **10**, Article No. 2522. https://doi.org/10.1038/s41467-019-10552-y

[7] Werthamer, N.R., Helfand, E. and Hohenberg, P.C. (1966) Temperature and Purity Dependence of the Superconducting Critical Field, H_{c2}III Electron Spin and Spin-Orbit Effects. *Physical Review*, **147**, 295-302. https://doi.org/10.1103/PhysRev.147.295

[8] Talantsev, E.F. (2019) Classifying Superconductivity in Compressed H_3S. *Modern Physics Letters B*, **33**, Article ID: 19501951. https://doi.org/10.1142/S0217984919501951

[9] Minkov, V.S., *et al*. (2022) Magnetic Field Screening in Hydrogen-Rich High-Temperature Super Conductors. *Nature Communications*, **13**, Article No. 3194. https://doi.org/10.1038/s41467-022-30782-x

[10] Minkov, V.S., Ksenofontov, V., Bud'ko, S.L., Talantsev, E.F. and Eremets, M.I. (2023) Magnetic Flux Trapping in Hydrogen-Rich High-Temperature Super Conductors. *Nature Physics*, **19**, 1293-1300. https://doi.org/10.1038/s41567-023-02089-1

[11] Malik, G.P. (2016) Superconductivity: A New Approach Based on the Bethe-Salpeter Equation in the Mean-Field Approximation. (Series on Directions in Condensed Matter Physics Book 21). World Scientific Publishing Co., Pte Ltd., Singapore. https://doi.org/10.1142/9868

[12] Malik, G.P. and Varma, V.S. (2020) Generalized BCS Equations: A Review and a Detailed Study of the Superconducting Features of $Ba_2Sr_2CaCu_2O_8$. In: Yavari, H., Ed., *On the Properties of Novel Superconductors*, Intech Open, London, 203.

[13] Malik, G.P. (2022) Superconductivity of Compressed H_2S in the Framework of the Generalized BCS Equations. *European Physics Journal Plus*, **137**, Article No. 786. https://doi.org/10.1140/epjp/s13360-022-03003-z

[14] Malik, G.P. and Varma, V.S. (2022) On the Temperature- and Magnetic Field—Dependent Critical Current Density of Compressed Hydrogen Sulphide. *Journal of Superconductivity and Novel Magnetism*, **35**, 3119-3126. https://doi.org/10.1007/s10948-022-06357-8

[15] Malik, G.P. and Varma, V.S. (2023) On the Generalized BCS Equations Incorporating Chemical Potential for the *Tc* and the Calculation of the Coherence Length of Some Elements and Compressed H_3S. *Journal of Low Temperature Physics*, **211**, 45-58. https://doi.org/10.1007/s10909-023-02938-6

[16] Eagles, D.M. (1969) Possible Pairing without Superconductivity at Low Carrier Concentrations in Bulk and Thin-Film Superconducting Semiconductors. *Physical Review*, **186**, 456-463. https://doi.org/10.1103/PhysRev.186.456

[17] Leggett, A.J. (1980) Cooper Pairing in Spin-Polarized Fermi Systems. *Journal des Physique Colloques*, **41**, C7-19-C7-26. https://doi.org/10.1051/jphyscol:1980704

[18] Malik, G.P. (2014) BCS-BEC Crossover without Appeal to Scattering Length Theory. *International Journal of Modern Physics B*, **28**, Article ID: 1450054. https://doi.org/10.1142/S0217979214500544

[19] Schrieffer, J.R. (1964) Theory of Superconductivity. WA Benjamin Publisher, Massachusetts. 41 p.

[20] Malik, G.P. and Varma, V.S. (2023) A Dynamical Approach to the Explanation of the Upper Critical Field Data of Compressed H_3S. *World Journal of Condensed Matter Physics*, **13**, 79-89. https://doi.org/10.4236/wjcmp.2023.133005

[21] Malik, G.P. and Varma, V.S. (2021) A New Microscopic Approach to Deal with the Temperature- and Applied Magnetic Field-Dependent Critical Current Densities of Superconductors. *Journal of Superconductivity and Novel Magnetism*, **34**, 1551-1561. https://doi.org/10.1007/s10948-021-05852-8

[22] Malik, G.P. and Varma, V.S. (2020) On a New Number Equation Incorporating Both Temperature and Applied Magnetic Field and Its Application to MgB_2. *Journal of Super-Conductivity and Novel Magnetism*, **33**, 3681-3685. https://doi.org/10.1007/s10948-020-05639-3

[23] Talantsev, E.F. (2020) Debye Temperature in LaHx-LaDy Superconductors. arXiv: 2004.03155.

[24] Malik, G.P. (2021) The Debye Temperatures of the Constituents of a Composite Superconductor. *Physica B*: *Condensed Matter*, **628**, Article ID: 413559. https://doi.org/10.1016/j.physb.2021.413559

Appendix A: Notation

(a_0, a_2): Constants in $q(t) = 1 + a_0\left(1 - t^2\right)^{a_2}$ which determines how the chemical potential varies via $\mu(t) = \mu_1 q(t)$, where μ_1 is the chemical potential at $t = 1$, *i.e.*, $T = T_c$

c: velocity of light

e: electronic charge

E_F: Fermi energy

$h = H_c/H_{c20}$, the reduced critical field

H_c: The applied critical magnetic field

H_{c1}: The lower critical magnetic field

H_{c2}: The upper critical magnetic field

H_{c20}: Assumed value of the upper critical field at $T = 0$

J_c: Critical current density

J_{c1}: Critical current density due to H_{c1}

J_{c2}: Critical current density due to H_{c2}

k: Boltzmann constant

m^*: Effective mass of an electron

m_e: Mass of a free electron

N: Demagnetizing factor

N_s: Number density of charge carriers

$\boldsymbol{p}$: Relative momentum of the constituents of a Cooper pair in the center-of -mass frame

$\boldsymbol{P}$: momentum of a Cooper pair in the lab frame

$q = \mu(t)/\mu_1$

sf: Self-field

$t = T/T_c$, the reduced temperature

T: Temperature (also employed for Tesla, which is clear from the context).

T_c: Critical temperature

v_c: Critical velocity

v_F: Fermi velocity

$y = k\theta/\alpha$

$\alpha = |\boldsymbol{P}||\boldsymbol{p}|\cos(\boldsymbol{P}, \boldsymbol{p})/2m^*$

Δ: Energy gap

$\eta = m^*/m_e$, Effective mass parameter

$\theta = \theta_H$, Debye temperature of H ions in H_3S

$\theta(H_3S)$: Debye temperature of H_3S

θ_S: Debye temperature of S ions in H_3S

$\kappa = \lambda_L/\xi$, Ginsberg-Landau parameter

λ_L: London penetration depth

λ_m: Magnetic interaction parameter

λ_{m1}: Magnetic interaction parameter at $T = T_c$, *i.e.*, $t = 1$

μ: Chemical potential

μ_1: Chemical potential at $T = T_c$, *i.e.*, $t = 1$

ξ: Coherence length

$\rho = \mu_1/k\theta$

$\Omega(h) = \Omega_0 h H_{c20}/\eta$

$\Omega_0 = e/m_e c$

Appendix B: Flow Charts

1) *The* (a_0, a_2) *approach*:

Step 1: Set values of T_c, η and *sf*. Choose a value of ρ.

Step 2: For $T = T_c$ ($t = 1$), use (13) to solve for λ_{m1}.

Step 3: Select two pairs of data points (T, H_{c2}), use (13) to solve for (a_0, a_2).

Step 4: With (a_0, a_2) known, solve (13) to obtain the values of H_{c2} and μ at $T = 10$ K. Employ these to sequentially obtain the values of v_F, ξ, N_s, λ_L, κ, H_{c1} and, finally, J_{c1} via equations given in the text.

Step 5: If the above value of J_{c1} does not agree with the sought value, e.g., 1.87×10^9 A/cm^2 in the case of H&M, repeat the entire chain of calculations starting with a different value of ρ till the desired value of J_{c1} is obtained. Following this procedure, remarkably, we were led via $\rho = 0.164$ to not only the value of J_{c1}, but also of H_{c1} and λ_L which are in agreement with the H&M's values.

2) *The* (q, y) *approach*:

Step 1: Set the values of T_c, η and *sf*. Choose a value of ρ.

Step 2: For $T = T_c$ ($t = 1$), use (13) to solve for λ_{m1}.

Step 3: Employing as input the obtained value of λ_{m1} and the H&M's or the Minkov, *et al.*'s values of J_{c1} and H_{c1}, solve (13), with X, Y as in (16), and (20) simultaneously for q and y.

Step 4: Employing the equations given in the text, sequentially calculate the values of v_F, ξ and N_s, culminating with the value of λ_L.

Step 5: If the above value of λ_L does not agree with the sought value, repeat the entire procedure starting with a different value of ρ.

Remark: The above flow-charts bring out the role of $\mu = \rho k\theta$ as the predominant governor of several properties of the SC under study.